Special Section: HOBE

Casper Kirkegaard*
Torben O. Sonnenborg
Esben Auken
Flemming Jørgensen

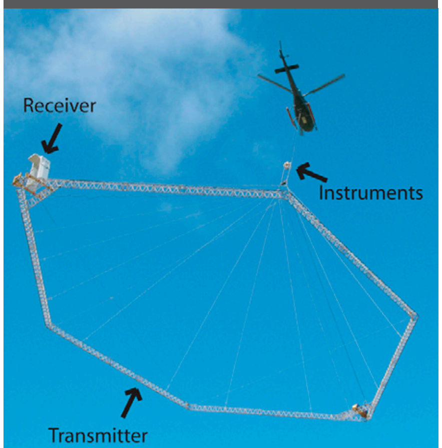

Understanding hydrogeologic processes in coastal areas is very important for, e.g., groundwater management and can be a very complicated task. Such settings are often governed by complex processes that can be very difficult to map. We demonstrated how airborne electromagnetic methods can be used to map the salinity distribution in such an area.

C. Kirkegaard and E. Auken, Dep. of Earth Sciences, Aarhus Univ., Hoegh-Guldbergs Gade 2, DK-8000 Aarhus, Denmark; T.O. Sonnenborg, Geological Survey of Denmark and Greenland, Oester Voldgade 10, DK-1350 Koebenhavn K, Denmark; and F. Jørgensen, Geological Survey of Denmark and Greenland, Lyseng Allé 1, DK-8270 Hoejbjerg, Denmark. *Corresponding author (casper.kirkegaard@geo.au.dk).

Vadose Zone J. 10:125–135
doi:10.2136/vzj2010.0038
Received 3 Mar. 2010.
Published online 20 Jan. 2011.
Open Access Article

Salinity Distribution in Heterogeneous Coastal Aquifers Mapped by Airborne Electromagnetics

Understanding the hydrologic setting of any given area is a challenging task, especially considering that the amount of available information is often very sparse relative to the size of the area and the complexity of the problem. We used geophysical transient electromagnetic (TEM) data from an airborne SkyTEM instrument to investigate discharge of freshwater from a river catchment into a coastal lagoon area, in support of large-scale hydrologic mapping of the HOBE hydrology research center. Existing hydrologic data indicate possible outflow from the catchment underneath the survey area, a hypothesis that was indeed backed up by our geophysical results. The results revealed a stratified geologic setting frequently incised by buried valleys beneath the lagoon. They also showed that the valleys are saturated with sea water, unlike the layers at the same depth that are probably saturated with brackish water. The salinity decreases with depth in large parts of the lagoon. The salinity distribution in the setting indicates the presence of intricate flow systems beneath the coastal area and the lagoon, and we propose that it is governed by the heterogeneity in the geologic setting. We also demonstrated how water depth as well as salinity can be accurately mapped using SkyTEM in combination with a robust and flexible inversion scheme.

Abbreviations: LCI, laterally constrained inversion; mbsl, meters below sea level; SCI, spatially constrained inversion; SGD, submarine groundwater discharge; TEM, transient electromagnetic.

Mapping the subsurface of the ground below shallow saline water using airborne electromagnetic methods is a challenging task and a topic that does not often appear in the literature. The relatively high conductivity of salt water tends to shield structures beneath it, often limiting geophysical information that can be extracted from the data. Airborne frequency domain methods have been widely used (e.g., Siemon et al., 2007; Fitterman and Deszcz-Pan, 1998; Siemon et al., 2009) but only for mapping the fresh–saltwater boundary, not to map below it. Ground-based TEM instruments have been used for saltwater boundary mappings by, e.g., Kafri and Goldman (2005), Nielsen et al. (2007), and Sørensen et al. (2001), and similar studies were done by d'Ozouville et al. (2008) using airborne TEM. Recent studies by Vrbancich (2009) revealed certain geological structures underneath seawater, using a specialized SeaTEM instrument.

Mapping of fresh water below the saltwater boundary has been done in a recent study in the Venice lagoon, Italy (Viezzoli et al., 2010). In this study, we used the same airborne system, SkyTEM (Sørensen and Auken, 2004) but configured for an even greater depth of investigation. We also used a more sophisticated regionally tuned starting model in the inversion, allowing shallow water to be accurately resolved. A byproduct of the mapping is a map of water salinity and a bathymetry map accurate to within a few meters, which is close to what was reported from more specialized bathymetry studies by, e.g., Vrbancich and Fullagar (2007) and Vrbancich (2009, 2010).

In this study, we performed a SkyTEM survey over the very shallow Ringkøbing fjord, a lagoon in western Denmark (Fig. 1). Along with important technical results, the geophysical results of the survey were related to the large-scale geologic and hydrologic setting of the area. The study was motivated by the need to assess the water budget of the HOBE catchment (Jensen and Illangasekare, 2011). Submarine groundwater discharge (SGD) to the sea (Burnett et al., 2006) was expected to be a relatively small part of the total freshwater outflow from the catchment; however, its contribution may be important when closing

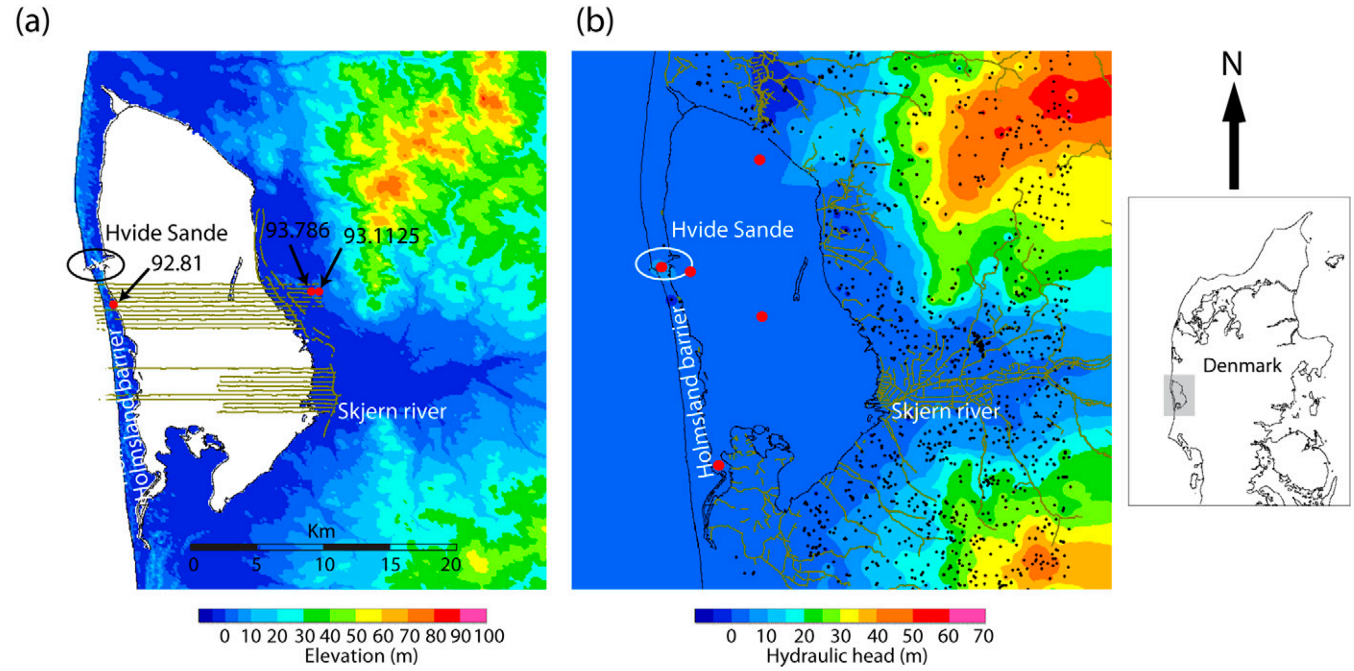

Fig. 1. Survey area overview: (a) topographical map, with red markers indicating deep boreholes used for the interpretation and olive lines marking the positions of the SkyTEM soundings; and (b) hydraulic head map, with black markers indicating positions of the head measurements, red markers indicating positions of salinity profile measurements, and olive lines marking the streams in the area.

the water balance. Our objective was to map the large-scale salinity distribution of the coastal aquifers and, in combination with hydrogeologic information, to localize areas prone to high SGD and to estimate the most important drivers of SGD that should be taken into account in subsequent analyses of groundwater discharge rates in the area.

Applied Methods and Survey

Geophysical Methodology

The survey was flown using a state of the art SkyTEM system (Fig. 2). SkyTEM is a helicopter-borne time domain electromagnetic system specifically designed for hydrogeophysical and environmental investigation purposes. During operation, the system continuously records raw data soundings, laser altitude readings, geographic positioning system positions, and instrument pitch and roll for further processing and inversion. The TEM soundings are acquired alternating between two transmitter magnetic moments: a low moment for resolving near-surface structures and a high moment for resolving deeper layers.

An implicit assumption when working with TEM data is that the resistivity of the ground is isotropic. Because the TEM method provides a resistivity measure based on only horizontal flowing currents, we cannot estimate the coefficient of vertical/horizontal anisotropy. Based on the investigation of a larger number of Ellog drillings (Sørensen and Larsen, 1999), however, we know that the coefficient of anisotropy is typically between 1.0 and 1.3 for Danish sediments (Christensen, 2000; Christensen, personal communication, 2010). A factor of this size is not significant for the overall conclusions drawn in this study.

Processing of the data was done in the Aarhus Workbench (Auken et al., 2009b), a modular software suite for processing, inverting, and visualizing geophysical data in a geographic information system (GIS) environment. The SkyTEM module used for processing includes application of instrument calibration parameters, correction for pitch and roll of the instrument, as well as filtering of the altitude readings. The details of the processing workflow were described in Auken et al. (2009a).

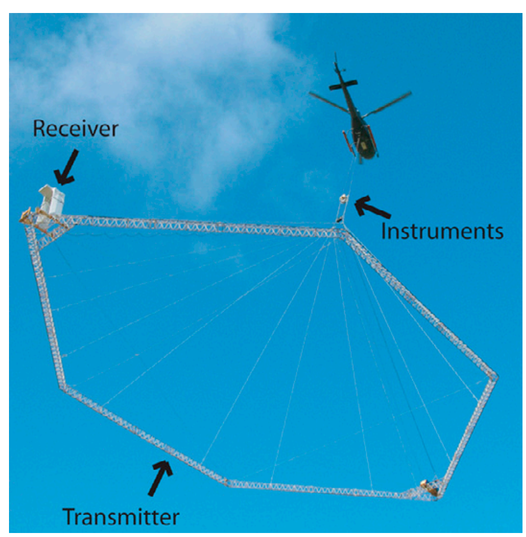

Fig. 2. The SkyTEM instrument in operation.

For inversion of the processed data, the code em1dinv (Christiansen and Auken, 2008) was used, which is the inversion kernel in the Aarhus Workbench. The code is based on a local, one-dimensional, forward response and the idea of constraining neighboring model parameters to each other by covariance and roughness matrices. When model parameters are constrained between neighboring models along the flight lines, it is termed *laterally constrained inversion* (LCI) (Auken et al., 2005); when model parameters are further constrained to the neighboring models of adjacent lines, it is termed *spatially constrained inversion* (SCI) (Viezzoli et al., 2008). Adding constraints to the inversion makes it possible to resolve features that would not be seen in an independent inversion, i.e., LCI and SCI can be seen as quasi-two- and -three-dimensional schemes, improving lateral and spatial resolution, respectively. The code is able to invert for instrument altitude in both LCI and SCI modes and provides means for carefully controlling the change in this parameter during inversion iterations.

One particularly appealing reason for choosing the combination of the Aarhus Workbench SCI module and em1dinv as an inversion tool is its ability to properly invert data collected in areas with very widely and rapidly varying target resistivities. For such data sets, convergence issues are common when using a simple uniform starting model and when the change of, for example, altitude is not carefully controlled during the iterations of the inversion. When inverting data acquired in an area with large resistivity variations, e.g., partly onshore and partly offshore, choosing a good uniform starting model for the entire survey can be difficult. To accommodate both highly resistive and highly conductive structures, the only viable choice of starting model is one of medium resistivity if convergence is to be assured. Choosing such a compromise starting model can work well; however, if additional parameters such as instrument altitude are included in the inversion, it can cause equivalence-like problems. When the initial resistivity of the top layer is much higher than the actual resistivity, and altitude is included in the inversion, there is a common tendency for the top model layer to be artificially included in the highly resistive air layer between the instrument and the ground. The result is that the top layer resistivity becomes very high and the instrument altitude is lowered, effectively extending the air layer into the ground. Such problems can be resolved by modifying the starting model to better match the distinct areas of a survey and controlling the change in model parameters during the inversion. For this study, we used Aarhus Workbench for producing a nonuniform starting model directly from a GIS map and kept the altitude constant in em1dinv for the first 10 iterations. This approach ensured that the actual resistivity structure was determined reasonably well before the instrument altitude was allowed to change, thereby solving the problem.

The investigation area is seen in Fig. 1 and is located on the western coast of Denmark. The survey consisted of 350 line kilometers flown in an east–west direction over the Ringkøbing lagoon with a flight line spacing of around 300 m. This spacing was chosen to maximize the spatial coverage of the survey while at the same time maintaining the ability to resolve the extent of relatively small geologic features. In this particular survey, the helicopter flew at an average speed of around 13 m/s. The transmitter was set up for low and high transmitter moments of 5000 and 179,000 A m^2, respectively, allowing measurement of 20 unbiased, logarithmically spaced gates in the interval 11.7 to 450 μs for the low moment and 21 gates in the interval 94 μs to 8 ms for the high moment. To assure consistent data quality, the instrument was calibrated to a reference model at the Danish national test site before the survey and the calibration was routinely validated throughout the survey.

During data processing, couplings to artificial conductors were manually removed from the raw data before averaging, for a resulting sounding approximately every 30 m. The resulting data were inverted using the LCI and SCI schemes for both variable and fixed layer boundary models. The results presented here are two SCI inversions: a 19-layer inversion using fixed layer boundaries and a five-layer result with variable layer boundaries. These two types of inversions produced the same overall resistivity pattern and were used complementarily. For a fixed boundary inversion with many layers, a smoothly varying resistivity model is obtained, whereas a discrete inversion using fewer layers and variable layer boundaries allows sharp layer boundaries to be resolved. The starting model of the inversions was set up to be locally uniform in the three geologically distinct areas of the survey, i.e., over the sea, over the lagoon, and over land.

General Survey Area Description

Ringkøbing lagoon is situated between the Skjern River system to the east and the Holmsland Barrier to the west. It has a coastline of approximately 110 km and an area of approximately 300 km^2. The shallow lagoon is connected to the North Sea through a sluice at Hvide Sande on the Holmsland Barrier and has an average depth of 1.9 m (Ringkøbing Amt, 2004). The deepest point is 5 m but more than 25% of the area is characterized by a depth <0.5 m. The total water volume is approximately 560 million m^3 and the residence time is on the order of 3 to 4 mo. The sluice is operated such that the water level in the lagoon is below 0.25 m above mean sea level. In situations when high water levels in the North Sea are combined with high river flow, however, this target level may be exceeded. The area surrounding the lagoon is relatively flat, with a land surface elevation generally below 30 m above sea level (Fig. 1).

During the Late Weichselian, the eastern part of Denmark was covered by glaciers while large outwash plains were formed in large parts of the ice-free western part of Jutland. The area was subsequently covered by the sea during the Holocene Transgression (Anthony and Møller, 2002). Approximately 5000 yr ago, the relative sea level in the area reached the present conditions. At that time, the coastline was situated at the outlet of Skjern River and the Ringkøbing lagoon area was a part of the North Sea. Since then, the Holmsland Barrier was created by strong sediment transport processes parallel to the west coast of Jutland. It is estimated that the lagoon became isolated from the North Sea in the 17th or 18th century, resulting in a significant reduction in its salinity. Since then, it has been characterized as a lagoon with brackish water.

Geology

The sedimentary setting is composed of three major sequences. A deep marine Paleogene clay with very low resistivities (1–5 Ω m; Jørgensen et al., 2005) constitutes the lower sequence. This is situated at depths of around 300 m in the area (Friborg and Thomsen, 1999). The Paleogene clay is followed by alternating layers of Miocene sand, silt, and clay (Rasmussen, 2004; Scharling et al., 2009) with resistivities above 20 to 30 Ω m, provided that the pore water is not saline (Jørgensen and Sandersen, 2009a). The Miocene sequence is covered by a relatively thin sheet of glacial sediments (10–20 m), but in places where tunnel valleys incise the Miocene, the glacial sediments can be considerably thicker (Jørgensen and Sandersen, 2006). The glacial setting is mainly composed of coarse meltwater sediments with resistivities above 100 to 200 Ω m (fresh pore water) (Jørgensen and Sandersen, 2009a). Occasionally, clayey tills and glaciolacustrine clay also occur within the glacial sequence.

Hydrology and Hydrogeology

The Ringkøbing lagoon is recharged by the Skjern River and two smaller streams covering a total catchment area of 3500 km^2. The annual mean river outflow to the lagoon amounts to approximately 50 m^3/s. Average precipitation and evaporation from the lagoon amounts to approximately 10 and 6 m^3/s, respectively, with evaporation ranging from approximately 16 m^3/s during the summer to insignificant values during the winter. It is expected that the lagoon is recharged by groundwater from the upstream catchment; however, the quantity of this component is not known. Unfortunately, no measurements are available on the quantity of water discharging through the sluice and it is therefore not possible to estimate the groundwater inflow by mass balance.

Hydraulic head measurements sampling the unconfined aquifer in shallow wells are available from the area and, based on a contour map of the heads (Fig. 1b), it was found that groundwater flows toward the lagoon. The hydraulic gradients are perpendicular to the coast both north and south of the Skjern River, with relatively small gradients close to and in the lagoon area. Only a few measurements of hydraulic head from filters located deeper than 30 m below mean sea level (mbsl) are available and do not support the construction of a potential head map. A measurement from a deep filter located at 150 mbsl in a new deep well installed at the east side of the lagoon (Jupiter archive no. 93.1125, jupiter.geus.dk/cgi-bin/svgrapport.dll?borid=431901&format=pdf, verified 28 Nov. 2010) (see Fig. 1a), however, shows a head value of 6.2 m above sea level (1.2 m above ground level). At this point, the hydraulic head of the shallow groundwater is between 3 and 5 m above sea level, indicating that vertical gradients between the deeper aquifers and the shallow groundwater exist. Hence, upward groundwater seepage from the deep-seated aquifers toward the lagoon may take place. Neither the geology nor the hydrogeology in the area is well mapped, however, and there is therefore a substantial degree of uncertainty with respect to the exchange between deep and shallow groundwater.

The exchange of water between the lagoon and the North Sea is controlled by the sluice at Hvide Sande, established in 1931. The sluice is operated such that the salinity in the lagoon is within predefined levels. Because of eutrophication problems caused by high inputs of nutrients from the upstream agricultural catchment, it was decided to increase the salinity in the lagoon in the late 1980s. Since then the sluice has been operated such that the salinity is kept between 6 and 15 g/L. To accurately control the salinity in the lagoon by sluice operation, a salinity observation network has been established (Nielsen et al., 2005). Weekly measurements of the Cl^- concentration using chlorine, temperature, and depth (CTD) instruments are performed according to the Helsinki Commission (2010). The salinity is monitored by collecting vertical salinity profiles at four different locations distributed within the lagoon (Petersen et al., 2008) and one by the sluice (see Fig. 1b). Significant seasonal variation in salinity has been observed, with low values, 6 to 7 g/L, during winter (January–April) and relatively high values, 10 to 13 g/L, during summer and autumn (June–October). The lagoon is exposed to strong westerly winds that ensure the water in the lagoon is generally well mixed; however, situations with vertical stratification are found when the sea water with a salinity of 33 g/L is let in from the North Sea through the sluice. This condition only exists at wind speeds below 8 m/s, beyond which full mixing takes place. At the time of the survey the average salinity in the lagoon was measured at 13.2 g/L. This value was obtained by a weighted average of samples from both deep and shallow water from the observation network stations.

Results

Geophysical Results

The outline of the resulting resistivity distribution in the survey area obtained by SCI inversion can generally be divided into three main areas: (i) the western part of the lagoon, where thick conductive layers cover the setting; (ii) the eastern part of the lagoon, where the setting is covered by thin conductive layers; and (iii) the onshore areas, where high resistivities generally prevail. When working with electromagnetic data, it is very important to consider the depth of investigation over the survey area, i.e., how deep the models provide useful information. In this particular survey area, the depth of investigation is strongly determined by the thickness of conductive layers shielding the lower lying structures. Based on a sensitivity analysis (Christiansen and Auken, 2010), we estimate that the models are generally trustful down to a depth of around 150 m in the western part of the lagoon, 200 m in the eastern part of the lagoon, and 300 m for onshore areas.

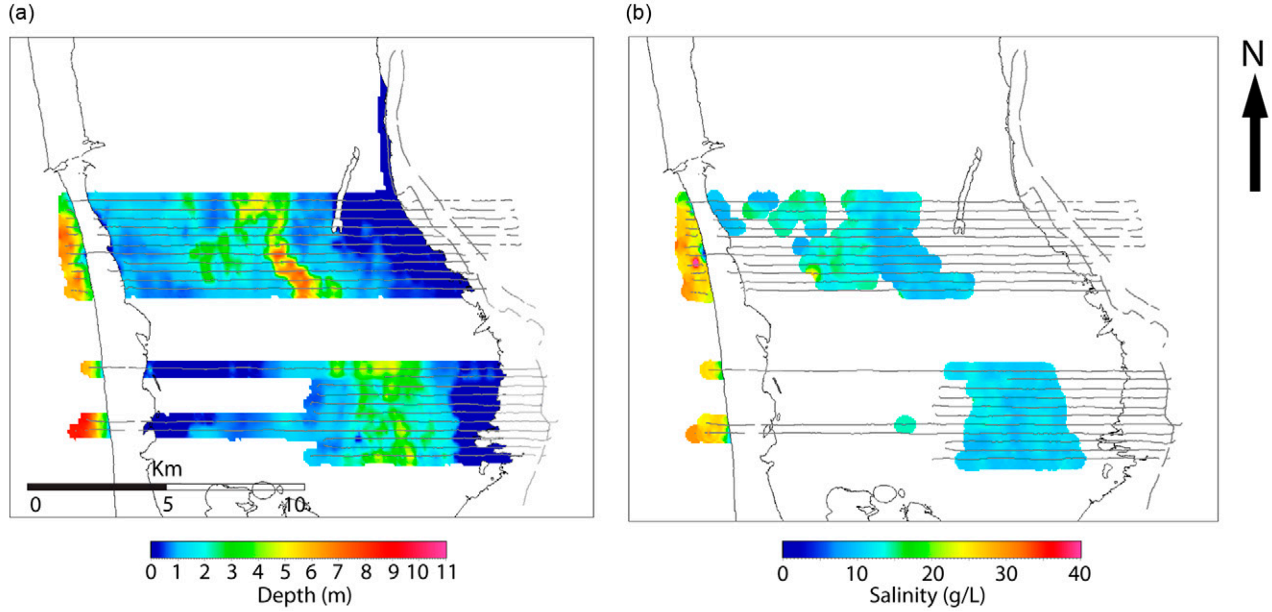

Fig. 3. Maps extracted from the five-layer spatially constrained inversion: (a) bathymetry map with an estimated accuracy of around 2 m; and (b) salinity map derived from resistivity.

When working with TEM data, it is implicitly assumed that the resistivity of the ground is isotropic. The TEM method provides a resistivity measure based on horizontal flowing currents only and cannot estimate the coefficient of anisotropy. Based on the investigation of a larger number of Ellog drillings (Sørensen and Larsen, 1999), we know that the coefficient of anisotropy typically is between 1.0 and 1.3 in Danish sediments (Christensen, 2000; Christensen, personal communication, 2010); however, a factor of this size is not significant for the overall conclusion drawn from this study.

Apart from mapping the substratum, the SkyTEM data provided information on both water depth and resistivity or salinity of the lagoon water (Fig. 3). The water depth map in Fig. 3 is based on the depth to the top of the first layer with a resistivity >0.7 Ω m. This map compares well to another water depth map by Nielsen et al. (2005) even though our depth generally tended to be a little greater. We estimate the depth map to be accurate within 2 m. The salinity map (Fig. 3) shows the salinity of the water in areas with a water depth of >2 m. In parts of the lagoon where the water layer is very thin, its exact properties could not be properly resolved and all we got from the inversion is that the top layer is very thin with a low, undefined resistivity. The salinity map was created by converting the resistivity of the top low-resistive layer into salinity. The conversion was based on a resistivity–salinity curve for water at 20°C by Keller and Frischknecht (1966). This curve is almost linear on a log–log plot for relevant salinity levels, making it a good approximation to extract the functional behavior from two data points (50 Ω m at 0.1 g/L and 0.65 Ω m at 10 g/L). The salinity levels found in the fjord area typically range from 10 to 15 g/L, with a tendency toward slightly increasing salinity levels in the western part of the fjord closest to the sluice to the North Sea. This range compares very well to the actual salinity level, which was measured at an average value of 13.2 g/L at the time of the campaign. In the survey area over the North Sea, the salinity levels are typically found between 25 and 32 g/L, which is also consistent with the known salinity level: an average salinity of 33 g/L with a tendency toward slightly lower levels near the coast.

Geologic and Hydrologic Interpretation

A high-resolution reflection seismic profile along the eastern coast of the Ringkøbing lagoon shows that the Miocene setting is relatively homogeneous in its structural appearance and that its setting is strongly stratified (Fig. 4). According to a couple of deep drillings in the northeastern part of the survey area (Jupiter archive no. 93.1125 and 93.786, jupiter.geus.dk/cgi-bin/svgrapport.dll?borid=74049&format=pdf, verified 28 Nov. 2010) (see Fig. 1), the setting is mainly composed by clay layers frequently intervened between silt and sand layers. In Fig. 5 it can be further seen through logs how resistivity relates to lithology in Borehole 93.1125 in the onshore part of the survey. In this borehole, the resistivity was found to be >20 Ω m for all types of sediments. For the quaternary sand and clays, the normal log shows resistivities around 100 to 200 Ω m, whereas the Miocene clay was found to have a resistivity around 20 to 50 Ω m and for Miocene sand >100 Ω m.

Figure 6 shows the average resistivities across four selected elevation intervals as extracted from the 19-layer models. It can be seen that the Miocene sequence in the area around the seismic line is imaged by a mixture of resistivities in all four intervals, with resistivities typically ranging from 30 to 100 Ω m. This is consistent with the resistivity levels expected for the Miocene

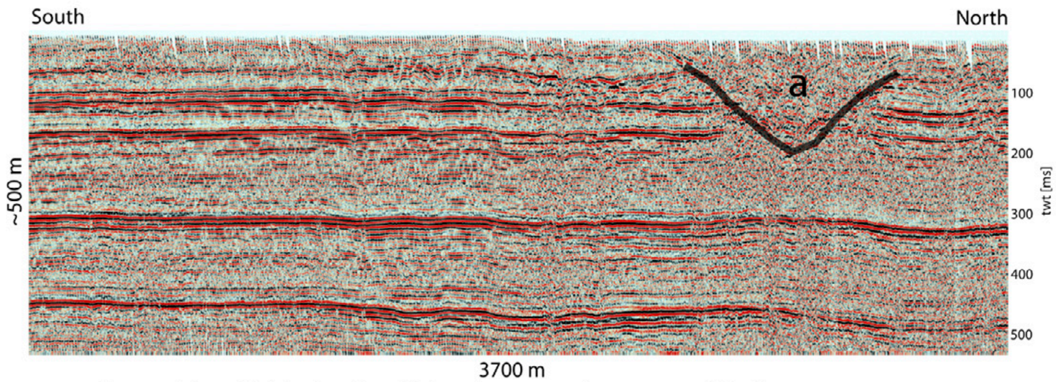

Fig. 4. High-resolution reflection seismic profile, showing a generally stratified Miocene setting incised by a buried tunnel valley (a).

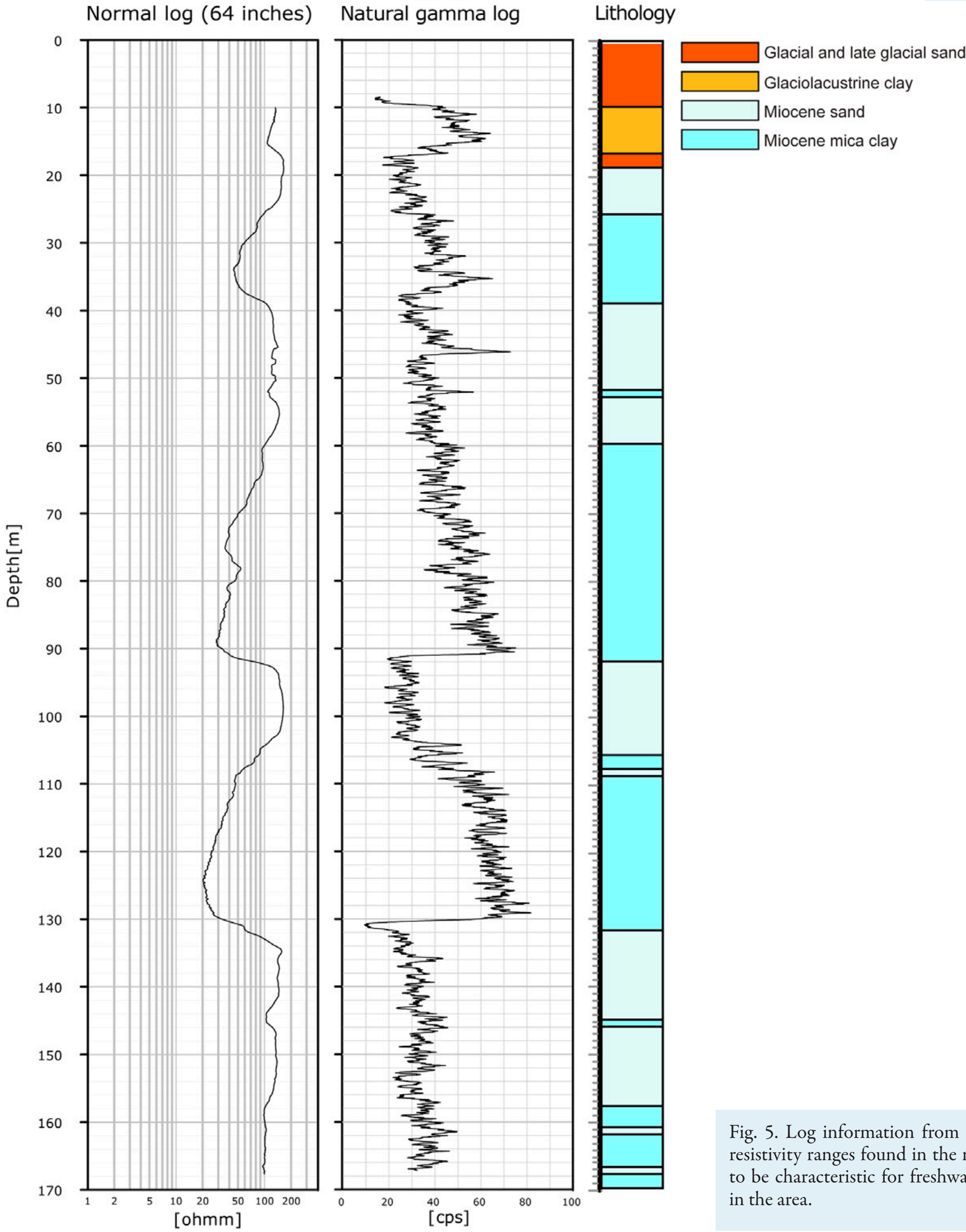

Fig. 5. Log information from Borehole 93.1125. The resistivity ranges found in the normal log are expected to be characteristic for freshwater-saturated sediments in the area.

sediments (Jørgensen and Sandersen, 2009a). The slight vertical changes are probably the result of a shifting dominance of clayey over sandy or silty sediments, whereas the lateral changes may be a result of facies variations within some of the thickest layers. It also can be seen in the seismic line that the Miocene setting is interrupted by a large incision from above. This is seen in the northern part of the section (denoted *a* in Fig. 4). Here, the Miocene setting appears to be incised down to at least 200-ms two-way time and, if a velocity of 1800 to 2000 m/s (Nielsen and Japsen, 1991) is used for depth conversion, the depth of the incision is at least 180 m. The appearance of the incision is typical for a buried tunnel valley in the area (Jørgensen and Sandersen, 2006, 2009a). The valley is situated in the northern part of the survey area denoted *a* in Fig. 6. It correlates with a low-resistive unit found in the TEM data along the two north–south-oriented flight lines. The low-resistive unit, which is oriented perpendicular to the coastline, was therefore assumed to be the response of the buried tunnel valley as seen in the seismic section. Buried tunnel valleys in Denmark are often filled with glaciolacustrine clay, which in freshwater-saturated environments can produce resistivities as low as about 20 Ω m (Jørgensen and Sandersen, 2009a); but the resistivities in the core of the unit (at depths of about 75 mbsl) were as low as 1 to 3 Ω m. Such conductive sediments are not found elsewhere in buried tunnel valleys unless the valley infill sediments are infiltrated by saline pore water. Thus, the very conductive response was, at least partly, caused by saline groundwater captured in the valley infill sediments.

The same reasoning was applied to the main part of the offshore survey area, where low to very low (typically <<15 Ω m) resistivities were seen from sea level and, in large parts of the area, down to the maximum penetration depth of the SkyTEM soundings. Especially at shallow depths, where resistivities showed mean resistivity levels of about 3.5 Ω m (Fig. 6, 10–20 mbsl), saline groundwater was expected to be present. Resistivity values at this low level may also represent Paleogene clay but this is situated at considerably greater depths (about 300 m). Freshwater-saturated glacial or Miocene sediments with a resistivity level like this have never been found in Denmark, despite the fact that >11,000 km^2 have been mapped by the TEM method and >1475 boreholes have been logged with resistivity tools (Møller et al., 2009). This is also supported by the resistivities presented in Fig. 5, where values above 20 Ω m are shown for the entire Miocene sequence.

In the 10 to 20 mbsl resistivity map, large parts of the shoreline along the eastern coast of the lagoon are seen to match exactly with the occurrence of saline groundwater. In some places, however, saline groundwater occurs behind the shoreline in a few low-lying areas that probably have been inundated during the Holocene transgression.

Moving further downward, a characteristic pattern becomes present within the expected low-resistive saltwater-saturated sediments. A series of conspicuous elongate structures are found with resistivities lower than their surroundings. These structures are generally between 1 and 2 km wide and are followed for at least 6 km in length. The overall pattern of the structures is very similar to the buried tunnel valleys described in the close vicinity of the survey area and elsewhere in Denmark and the North Sea (Jørgensen and Sandersen, 2006, 2009b; Huuse and Lykke-Andersen, 2000). They were therefore also interpreted as buried tunnel valleys. One tunnel valley striking southwest to northeast may be the correlating counterpart to the tunnel valley found onshore (*a*). In the 60 to 70 mbsl resistivity map, the valleys appear with very low resistivities. Apparently, they have conductive cores with resistivities around 1.75 Ω m. According to a 90-m-deep borehole (Jupiter archive no. 92.81, jupiter.geus.dk/cgi-bin/svgrapport.dll?borid=233818&format=pdf, verified 28 Nov. 2010) that penetrates the core of the northwesternmost tunnel valley, the core is composed of glacial sand. Thus, if the valley infill is composed of sand and a formation factor of 6 is expected to be valid for the sand (Kirsch, 2006), the specific resistivity of the groundwater must be 0.30 Ω m (Archie, 1942), close to that of the North Sea salt water. The valleys may therefore contain saline sea water rather than infiltrated brackish water from the lagoon. Miocene sediments between the valleys show resistivities of about 4 Ω m at the same level. This is a considerably higher resistivity than that measured in the tunnel valleys, and the Miocene sediments are therefore not expected to be infiltrated with seawater of the same salinity as that in the valleys. Furthermore, some of the electrical conductivity measured in the Miocene sediments originated from the clay layers within the Miocene, leaving a smaller contribution to originate from the ion content of the groundwater. This indicates that the salinity within the valleys is greater than that of the Miocene sequence, and a laterally differentiated distribution of the groundwater salinity appears throughout the area.

Further downward, the setting gradually becomes more resistive. The resistivity here is generally between 10 and 15 Ω m, but it is uncertain to what depth the SkyTEM soundings actually penetrated. The conductive setting acted as a prominent shield in areas where this setting is thickest. There is no doubt, however, that the resistivity generally increases at around 100 to 150 mbsl. This indicates a decrease in groundwater salinity.

Especially one area in the lagoon differs from the above description. This is found just off the shoreline in the northeastern part of the area, denoted *b* in Fig. 6 and 7. It gradually appears as a resistive area from around 30 mbsl. The resistivity patterns and values in the area below 30 m are comparable to those onshore; the sediments here were therefore interpreted to be freshwater saturated. A buried tunnel valley was interpreted to cross-cut the area, showing high resistivities corresponding to sandy infill sediments—here without saline groundwater.

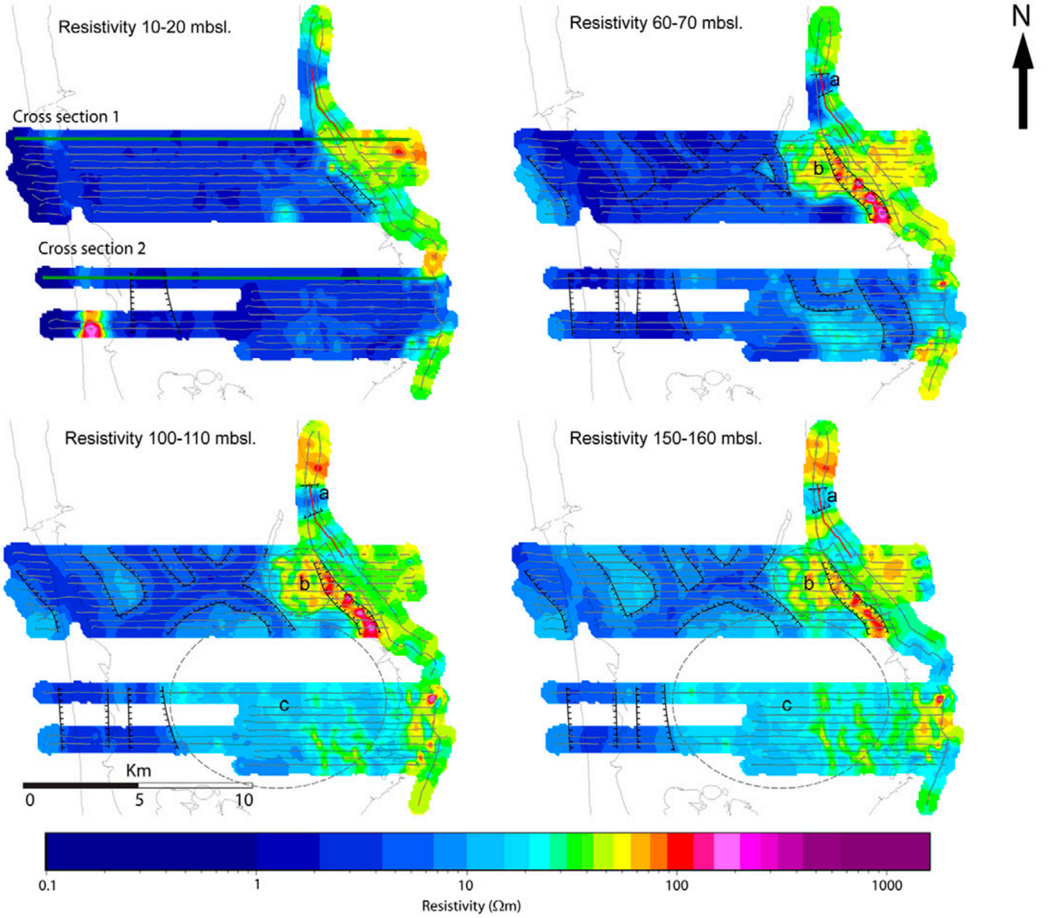

Fig. 6. Average resistivity maps across selected intervals. Buried tunnel valleys are outlined on each map. An incision in the Miocene setting is seen in area *a*, *b* indicates freshwater-saturated sediments, and *c* is an area of fresh and saline water mixing. The red line indicates the position of the seismic profile and the green lines the positions of the cross-sections.

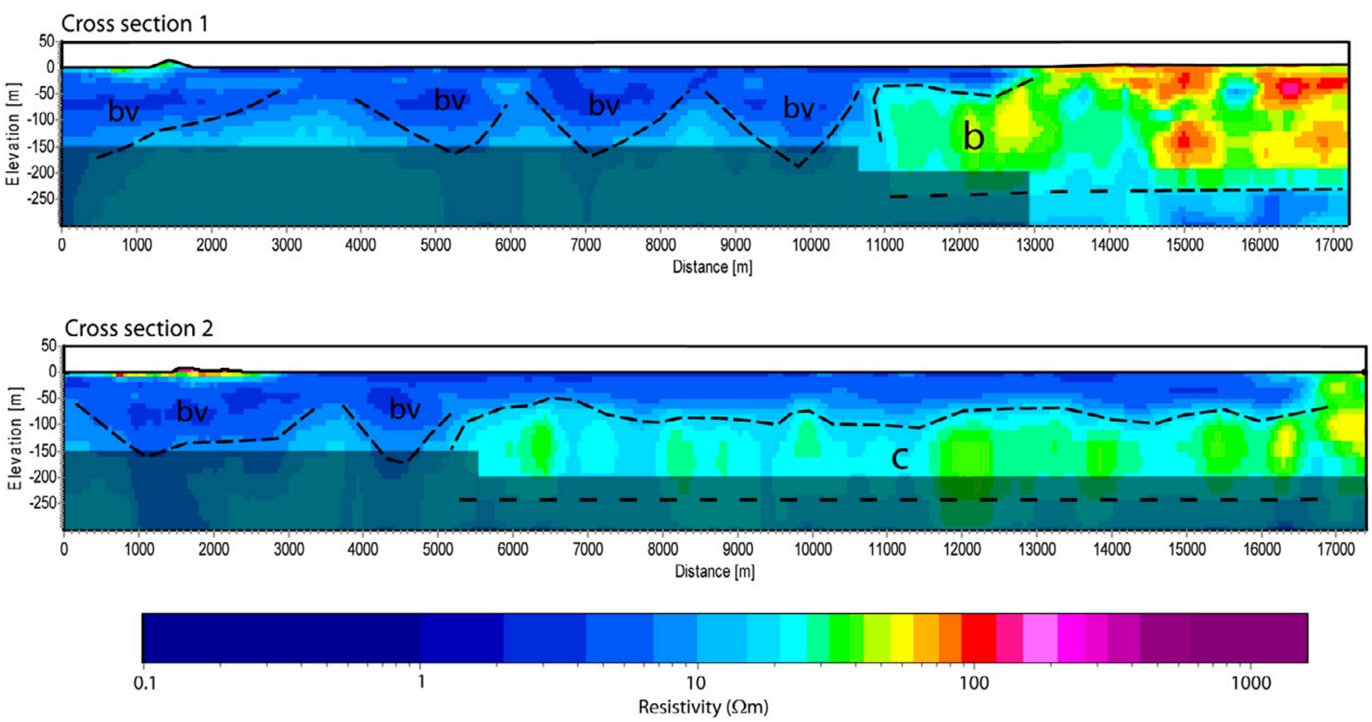

Fig. 7. Two vertical cross-sections oriented west–east across the survey area; *b* and *c* denote sub-lagoon layers infiltrated by fresh or brackish groundwater from the upstream catchment, and *bv* denotes the position of buried tunnel valleys saturated by groundwater with a high salinity. Interpretations and tentative interpretations are marked with broken lines. The deeper part of the substratum that is not or is only poorly resolved is shaded.

On the onshore part of Cross-section 1 in Fig. 7, a deep-seated conductive layer is found at depths of around 230 m. This is expected to be residual saline groundwater, because the otherwise very conductive Paleogene clay, which also produces a conductive response, is situated at greater depths. Information at this depth was only achieved because there was no or only very little shielding saline groundwater above. The lower saltwater boundary can be followed for some distance into the lagoon (until profile coordinate 11,000 m), but when the setting with saline groundwater above became too thick (to the west of area *b*), there was no longer any deep penetration. This boundary is likely to be present in the entire survey area.

Area *c* in Fig. 6 and 7 is characterized by an undulating signature of low to medium-low resistivities below the level of around 70 mbsl. Buried tunnel valleys that cross the area are marked in the 60 to 70 mbsl resistivity map in Fig. 6 but it is difficult to clearly discern whether they incise the deeper levels. A series of conspicuous elongate resistive features also emerges in the southeast part of the *c* area. It is likely that these features also can be interpreted as buried tunnel valleys. The entire *c* area is not comparable to the onshore areas despite the expectation of unchanged geology across the shoreline. Elevated salinity of the groundwater is a probable reason for this difference, and brackish groundwater could be present here. This layer of brackish groundwater is bounded upward at 60 to 70 mbsl and downward deeper than 150 mbsl (the depth of investigation) by more saline groundwater.

Discussion

Based on our investigations, the hydrogeologic setting of the investigated area is complex. The geology is dominated by stratified Miocene deposits with a homogeneous structural appearance of alternating layers of medium-permeability sands and low-permeability clays. Several tunnel valleys cross-cut the Miocene sequence down to approximately 200 mbsl. Information on the valley infill sediments is sparse, however, based on a few wells; and based on knowledge from similar valley systems in western Jutland, the infill is expected to be dominated by high-permeability sands. No information on the connectivity between the Miocene and the buried valley sediments is available; however, because the boundary is erosive, good hydraulic contact is expected at the horizons where valley sand is in contact with Miocene sand. The area is bounded by the brackish lagoon at the surface and by the North Sea to the west. Hydraulic heads in the aquifers to the east of the lagoon indicate that groundwater from the upstream catchment discharges into the area; this issue is discussed below.

Before the Holmsland Barrier was formed, the North Sea coast was located at the eastern coast of the lagoon. It is probable that a saltwater wedge was established at that time at the location of the former coastline, separating an upper freshwater zone from a saltwater zone below. When the barrier isolated the area from the North Sea approximately 300 yr ago, the lagoon was created. It is probable that the lagoon has been characterized by brackish water with salinities significantly below sea water levels since then. Hence, it may be assumed that the salinity distribution below the lagoon has subsequently been in a transient state, where salt water is displaced by fresh water originating primarily from the Skjern River catchment. This requires that groundwater from the Skjern catchment discharges into the Ringkøbing lagoon.

Based on the resistivity distribution in the lagoon area, brackish groundwater is found in large parts of the shallow subsurface. Generally, the salinity below the lagoon decreases with depth, facilitating downward, density-driven flow of the brackish water from the lagoon. Smith and Turner (2001) showed that the stability of density-driven convective flow is a function of (i) the downward destabilizing buoyancy effects of density contrasts between the lagoon and the underlying aquifer, and (ii) the upward stabilizing influence of groundwater discharge. The hydraulic head in the deeper aquifers and, hence the upward gradient, are expected to decrease toward the west. The possibility of density-driven downward flow is therefore expected to increase with distance from the eastern coast of the lagoon. Smith and Turner (2001) also concluded, however, that geologic heterogeneity may dramatically influence the flow field.

At greater depths (100–60 mbsl), groundwater with relatively low salinity is found, especially in the southern part of the area (e.g., area *c* in Fig. 6 and 7). This was interpreted as groundwater from the upstream catchment that discharges toward the North Sea through the Miocene layered sequence due to head differences. Generally, salinity levels increasing toward the west are found and the resistivity distribution seen in Fig. 7 indicates that the freshwater does not reach all the way to the Holmsland Barrier or beyond. This may be due to the fact that the groundwater is gradually mixed with salt water, both from the downward leakage from the lagoon and from deeper residual seawater. The discharge of fresh groundwater that is gradually being salinized as it flows toward the west may also escape through layers that are situated too deep to be captured by the instrument due to the limited depth of investigation. This possibility is supported by the fact that Miocene deposits in western Jutland are known to generally dip toward the southwest (Scharling et al., 2009).

The buried valleys in the area were, contrary to the Miocene sediments, interpreted to contain water with seawater salinity. The origin of this water may be old residual seawater that has not been flushed by discharging fresh water. Alternatively, the high salinity in the valleys could be caused by saltwater intrusion from the North Sea. The high-permeability valleys are in direct contact with the North Sea area, and sea water intrusion may therefore have caused the presence of water with high salinity. The hydraulic gradient of the fresh water in the area surrounding the Ringkøbing lagoon is relatively low (Fig. 1b) and the salt water may therefore be able to invade the valleys.

Interpretation of the flow system in the area is complicated by the historical changes in sea level and location of the coastline. During the Litorina transgression approximately 7000 yr BP, the sea level reached higher levels than presently with a coastline located to the east of Ringkøbing fjord. During the following regression that resulted in present-day sea levels approximately 5000 yr BP, displacement of salt water from especially the high-permeability sediments is assumed to have taken place. Subsequently, the Holmsland Barrier was generated about 300 yr ago, resulting in a further withdrawal of the coastline to its present position. Hence, the system is expected to be in a transient state where salt water is displaced by fresh water. It is not possible, based on current information, to give an unambiguous explanation of the current distribution of salt water and fresh water in the area.

The knowledge obtained from this study suggests that SGD is driven by both head gradients and convection, whereas drivers such as the tide, waves, and currents are expected to be of minor importance since the lagoon is protected by the Holmsland Barrier and has a limited horizontal extent.

Apart from the geologic and hydrogeologic results, our studies included an important technical result: SkyTEM data can produce accurate maps of bathymetry and salinity (Fig. 3) in areas of shallow saline water, as long as the water depth is greater than a few meters. To resolve such shallow layering at the very surface, we used a regionally tuned starting model for the inversion over the three distinct areas of the survey. It is important to note that we did not include any constraints from prior information and that the starting model did not include any regional variations, i.e., the extracted information was actually resolved by the instrument and cannot be considered an inversion artifact resulting from a perfect starting model.

From the results in Fig. 3 and 6, it is evident that very small variations in resistivity can be resolved in the inversion, particularly when the target resistivity is within the levels characteristic for saline water. The ability to resolve such subtle differences suggests that the method could potentially be used for resolving layering within a water column, e.g., haloclines.

Conclusions

The presented models obtained from inversion of SkyTEM data give a detailed description of the groundwater salinity distribution below the lagoon survey area. Based on these models, the area is characterized by complicated and tightly coupled geologic and hydrologic settings, combining into a spatially complex groundwater salinity distribution including areas of fresh water, brackish water, and seawater.

Buried tunnel valleys are found beneath the lagoon with a resistivity signature indicating saturation by seawater. The water filling the buried valleys could be either residual seawater from before the lagoon was formed or could come from a direct connection to the North Sea.

A hypothesis of flow from the Skjern River catchment toward the North Sea through both shallow and deeper lying aquifers is supported by the geophysical results. Our results indicate outflow from a shallow aquifer in the eastern part of the lagoon and also reveal a deeper lying brackish aquifer for which the point of discharge is more uncertain because it is located near the detection limits of the instrument.

Additionally, it was demonstrated that accurate maps of both bathymetry and seawater salinity can be produced from data acquired with a calibrated SkyTEM instrument. Subtle differences in resistivity were resolved by the inversion, suggesting that the method could be used for mapping layered features within a water column, such as haloclines.

Acknowledgments

We thank Anne-Sophie Christensen for seismic data processing and Jens Würgler Hansen, Environmental Centre of Ringkøbing, for supplying salinity data from the Ringkøbing lagoon. We also thank Bjarke Roth for assisting with the SkyTEM data processing, Grethe Storgaard for her help with making the figures, and Aaron Davis and Anders Vest Christiansen for proofreading. This study was funded by the Villum Foundation.

References

Anthony, D., and I. Møller. 2002. The geological architecture and development of the Holmsland Barrier and Ringkøbing Fjord area, Danish North Sea coast. Geogr. Tidsskr. 101:27–36.

Archie, G.E. 1942. The electrical resistivity log as an aid in determining some reservoir characteristics. Trans. Am. Inst. Min. Metall. Pet. Eng. 146:54–62.

Auken, E., A.V. Christiansen, B.H. Jacobsen, N. Foged, and K.I. Sørensen. 2005. Piecewise 1D laterally constrained inversion of resistivity data. Geophys. Prospect. 53:497–506.

Auken, E., A.V. Christiansen, J.A. Westergaard, C. Kirkegaard, N. Foged, and A. Viezzoli. 2009a. An integrated processing scheme for high-resolution airborne electromagnetic surveys: The SkyTEM system. Explor. Geophys. 40:184–192.

Auken, E., A. Viezzoli, and A.V. Christiansen. 2009b. A single software for processing, inversion, and presentation of AEM data of different systems. *In* Int. Geophys. Conf., 20th, Adelaide, SA, Australia [CD-ROM]. 22–25 Feb. 2009. Aust. Soc. Explor. Geophys., Perth, WA, Australia.

Burnett, W.C., P.K. Aggarwal, A. Aureli, H. Bokuniewicz, J.E. Cable, M.A. Charette, et al. 2006. Quantifying submarine groundwater discharge in the coastal zone via multiple methods. Sci. Total Environ. 367:498–543.

Christiansen, A.V., and E. Auken. 2008. Presenting a free, highly flexible inversion code. p. 1228–1232. *In* Expanded Abstr., Society of Exploration Geophysics Annu. Meet., 78th, Las Vegas, NV. 9–14 Nov. 2008. SEG, Tulsa, OK.

Christiansen, A.V., and E. Auken. 2010. A global measure for depth of investigation in EM and DC modeling. *In* ASEG Ext. Abstr., Int. Geophys. Conf., 21st, Sydney, NSW, Australia [CD-ROM]. 22–26 Aug. 2010. Aust. Soc. Explor. Geophys., Perth, WA, Australia.

Christensen, N.B. 2000. Difficulties in determining electrical anisotropy in subsurface investigations. Geophys. Prospect. 48:1–19.

d'Ozouville, N., E. Auken, K.I. Sørensen, S. Violette, G. de Marsily, B. Deffontaines, and G. Merlen. 2008. Extensive perched aquifer and structural implications revealed by 3D resistivity mapping in a Galapagos volcano. Earth Planet. Sci. Lett. 269:518–522.

Fitterman, D.V., and M. Deszcz-Pan. 1998. Helicopter EM mapping of saltwater intrusion in Everglades National Park, Florida. Explor. Geophys. 29:240–243.

Friborg, R., and S. Thomsen. 1999. Kortlægning af Ribe formationen. Et fællesjysk grundvandssamarbejde. Tech. Rep. Ribe Amt, Ringkøbing Amt, Viborg Amt, Århus Amt, Vejle Amt, Sønderjyllands Amt.

Helsinki Commission. 2010. Manual for marine monitoring in the COMBINE Programme of HELCOM. Available at www.helcom.fi/groups/monas/CombineManual/en_GB/main (verified 12 Nov. 2010). Helsinki Commission, Helsinki, Finland.

Huuse, M., and H. Lykke-Andersen. 2000. Overdeepened Quaternary valleys in the eastern Danish North Sea: Morphology and origin. Quat. Sci. Rev. 19:1233–1253.

Jensen, K.H., and T.H. Illangasekare. 2011. HOBE: A hydrological observatory. Vadose Zone J. 10:1–7 (this issue).

Jørgensen, F., and P.B.E. Sandersen. 2006. Buried and open tunnel valleys in Denmark: Erosion beneath multiple ice sheets. Quat. Sci. Rev. 25:1339–1363.

Jørgensen, F., and P.B.E. Sandersen. 2009a. Buried valley mapping in Denmark: Evaluating mapping method constraints and the importance of data density. Z. Dtsch. Ges. Geowiss. 160:211–223.

Jørgensen, F., and P.B.E. Sandersen. 2009b. Kortlægning af begravede dale i Danmark, opdatering 2007–2009. Geol. Surv. of Denmark and Greenland, Copenhagen.

Jørgensen, F., P. Sandersen, E. Auken, H. Lykke-Andersen, and K.I. Sørensen. 2005. Contributions to the geological mapping of Mors, Denmark: A study based on a large-scale TEM survey. Bull. Geol. Soc. Den. 52:53–75.

Kafri, U., and M. Goldman. 2005. The use of the time domain electromagnetic method to delineate saline groundwater in granular and carbonate aquifers and to evaluate their porosity. J. Appl. Geophys. 57:167–178.

Keller, G.V., and F.C. Frischknecht. 1966. Electrical methods in geophysical prospecting. Pergamon Press, Oxford, UK.

Kirsch, R. 2006. Groundwater geophysics: A tool for hydrogeology. Springer-Verlag, Berlin.

Møller, I., H. Verner, V.H. Søndergaard, J. Flemming, E. Auken, and A.V. Christiansen. 2009. Integrated management and utilization of hydrogeophysical data on a national scale. Near Surface Geophys. 7:647–659.

Nielsen, L.H., and P. Japsen. 1991. Deep wells in Denmark 1935–1990: Lithostratigraphic subdivision. Ser. A, Vol. 31. Geol Surv. Denmark, Copenhagen.

Nielsen, L., N.O. Jørgensen, and P. Gelting. 2007. Mapping of the freshwater lens in a coastal aquifer on the Keta Barrier (Ghana) by transient electromagnetic soundings. J. Appl. Geophys. 62:1–15.

Nielsen, M.H., B. Rasmussen, and F. Gertz. 2005. A simple model for water level and stratification in Ringkøbing Fjord, a shallow, artificial estuary. Estuarine Coastal Shelf Sci. 63:235–248.

Petersen, J.K., J.W. Hansen, M.B. Laursen, P. Clausen, J. Carstensen, and D.J. Conley. 2008. Regime shift in a coastal marine ecosystem. Ecol. Appl. 18:497–510.

Rasmussen, E.S. 2004. Stratigraphy and depositional evolution of the uppermost Oligocene–Miocene succession in western Denmark. Bull. Geol. Soc. Den. 51:89–109.

Ringkøbing Amt. 2004. Basisanalyse del I: Karakterisering af vandforekomster og opgørelse af påvirkninger.

Scharling, P.B., E.S. Rasmussen, T.O. Sonnenborg, P. Engesgaard, and K. Hinsby. 2009. Three-dimensional regional-scale hydrostratigraphical modeling based on sequence stratigraphical methods. Hydrogeol. J. 17:1913–1933.

Siemon, B., A.V. Christiansen, and E. Auken. 2009. A review of helicopter-borne electromagnetic methods for groundwater exploration. Near Surf. Geophys. 7:629–646.

Siemon, B., A. Steuer, U. Meyer, and H.-J. Rehli. 2007. HELP ACEH: A post-tsunami helicopter-borne groundwater project along the coasts of Aceh, northern Sumatra. Near Surf. Geophys. 5:231–240.

Smith, A.J., and J.V. Turner. 2001. Density-dependent surface water–groundwater interaction and nutrient discharge in the Swan–Canning estuary. Hydrol. Processes 15:2595–2616.

Sørensen, K.I., and E. Auken. 2004. SkyTEM: A new high-resolution helicopter transient electromagnetic system. Explor. Geophys. 35:191–199.

Sørensen, K.I., F. Effersø, and E. Auken. 2001. A hydrogeophysical investigation of the Island of Drejø. Eur. J. Environ. Eng. Geophys. 6:109–124.

Sørensen, K.I., and F. Larsen. 1999. Ellog auger drilling: Three-in-one method for hydrogeological data collection. Ground Water Monit. Rem. 19:97–101.

Viezzoli, A., A.V. Christiansen, E. Auken, and K.I. Sørensen. 2008. Quasi-3D modeling of airborne TEM data by spatially constrained inversion. Geophysics 73:F105–F113.

Viezzoli, A., L. Tosi, P. Teatini, and S. Silvestri. 2010. Surface water–groundwater exchange in transitional coastal environments by airborne electromagnetics: The Venice Lagoon example. Geophys. Res. Lett. 37:L01402, doi:10.1029/2009GL041572.

Vrbancich, J. 2009. An investigation of seawater and sediment depth using a prototype airborne electromagnetic instrument system: A case study in Broken Bay, Australia. Geophys. Prospect. 57:633–651.

Vrbancich, J. 2010. Preliminary investigations using a helicopter time-domain system for bathymetric measurements in shallow coastal waters? Port Lincoln and Broken Bay, NSW, Australia. *In* ASEG Ext. Abstr., Int. Geophys. Conf., 21st, Sydney, NSW, Australia [CD-ROM]. 22–26 Aug. 2010. Aust. Soc. Explor. Geophys., Perth, WA, Australia.

Vrbancich, J., and P.K. Fullagar. 2007. Improved seawater depth determination using corrected helicopter time-domain electromagnetic data. Geophys. Prospect. 55:407–420.